Supporting Information

Embedded Homogeneous Ultra-fine Pd Nanoparticles within MOFs Ultra-thin Nanosheets for Heterogeneous Catalysis

Taolian Guo,[a, §§] Kaili Mo,[a,§§] Nannan Zhang,[a] LiPengcheng Xiao,[a] Wenlong Liu[b] and Lili Wen[a,*]

[a] Key Laboratory of Pesticide & Chemical Biology of Ministry of Education, College of

Chemistry, Central China Normal University, Wuhan, 430079, China.

E-mail: wenlili@mail.ccnu.edu.cn (L. L. Wen).

[b] College of Chemistry & Chemical Engineering, Yangzhou University, Yangzhou, 225002, China.

[§§] The authors contributed equally.

Experimental Section

Materials and Chemicals. The reagents and solvents applied were commercially available and employed without further purification. Polyvinylpoyrrolidone (PVP, MW 58,000), Palladium chloride (PdCl$_2$), Sodium borohydride (NaBH$_4$, 98%), N, N'-Dimethylformamide (DMF, 99.8%), Sodium chloride (NaCl, 99.5%) were purchased from Aladdin. 5-(4-pyridyl)-methoxyl isophthalic acid (5,4-PMIA, 99%) and tetrakis(4-pyridyloxymethylene) methane (TPOM) was synthesized according to the literatures. [1,2]

Instrumentation. All powder X-ray diffraction (PXRD) data were collected on a Siemens D5005 diffractometer using Cu Kα radiation (λ =1.5418 Å) and 2θ ranging from 5 to 50°. Transmission electron microscope (TEM) was performed on a FEI

Tecnai G2 F20 electron microscope operating at 200 kV. UV-Vis absorption spectra were recorded at room temperature in quartz cells of 1 cm path length using a DH-MINI-Deuterium halogen light source spectrophotometer. X-ray photoelectron spectroscopy (XPS) analysis was performed using a VG Scientific Escalab 250Xi-XPS photoelectron spectrometer with an Al Kα X-ray resource. The binding energies were calibrated by the C1s binding energy of 284.7 eV. Inductively coupled plasma atomic emission spectroscopy (ICP-AES) was recorded on Vavian 715-ES. The specific surface areas were calculated based on nitrogen sorption-desorption isotherms at 77K measured by a Quantachrome IQ$_2$ system. Before the analysis, the solvent-exchanged samples were obtained by soaking the as-made samples in methanol for 2 days, refreshing every 4 h. The methanol-exchanged samples (approximately 100 mg) were dried by supercritical carbon dioxide (SCD) to remove guest solvent molecules, yielding activated samples. The pore volumes and pore size distributions were obtained from the adsorption branches of isotherms by using the nonlocal density functional theory (NLDFT) model.

Synthesis of Bulk MOF-Ni. Bulk MOF-Ni was synthesized according to the reported method reported by our group.[3] A mixture of Ni(NO$_3$)$_2$·6H$_2$O (7.3 mg, 0.025 mmol), 5,4-PMIA (6.9 mg, 0.025 mmol), TPOM (11.1 mg, 0.025 mmol), 2 M HCl (1 drop), DMA (2 mL), and H$_2$O (1 mL) was heated in a Teflon-lined stainless vessel (25 cm^3) at 140 °C for 3 d, followed by cooling to ambient temperature. The resulting bright-green crystals of bulk **MOF-Ni** were recovered by filtration.

Synthesis of NMOF-Ni Nanosheets. NMOF-Ni Nanosheets was synthesized by surfactant-assisted method reported by our group.[3] In a typical procedure, Ni(Ac)$_2$ · 4H$_2$O (0.1 g, 0.4 mmol), 5,4-PMIA (0.1 g, 0.37 mmol), TPOM (0.1 g, 0.22 mmol), and PVP (0.5 g) were mixed in DMF (10 mL), which was stirred for 10 min and then heated at 150 °C for 0.5 h in air. Finally, **NMOF-Ni** as green nanosheets was collected.

Syntheses of Pd@NMOF-Ni and Pd@MOF-Ni. In a typical synthesis, 150 mg of **NMOF-Ni** was dispersed in 20 mL deionized water. Then, 1 mL of PdCl$_2$ aqueous

solution (8.4 mg, 0.047 M) was added, generating green crystalline solid, which was separated through filtration, and subsequently redispersed into 20 mL deionized water, followed by adding aqueous $NaBH_4$ (2 mL, 0.1 M). After further stirring for 0.5 h, the resultant dark **Pd@NMOF-Ni** nanocomposite was isolated and washed with water. The Pd NPs loading was determined by inductively coupled plasmas (ICP) up to $\approx 2.5\%$ for **Pd@NMOF-Ni** nanocomposite. For comparison, Pd NPs was also loaded on the bulky counterpart **MOF-Ni** *via* the same path to yield **Pd@MOF-Ni**, and the content of Pd NPs is $\approx 2.3\%$, similar to that of **Pd@NMOF-Ni**.

Catalytic Hydrogenation of Alkenes. To compare the catalytic activity of the **Pd@NMOF-Ni** and **Pd@MOF-Ni**, both of which were utilized as catalysts for the hydrogenation of styrene as a model reaction. In a typical procedure, ethanol (3.0 mL) and the catalysts (5.0 mg) were added to a 5 mL vial and dispersed ultrasonically. Styrene (0.8 mmol) was then added into the vial. Subsequently, the vial was transferred into the preheated stainless steel autoclave. The autoclave was sealed and purged with high-purity H_2 for several times, and the final H_2 pressure of the autoclave was set at 0.1 MPa with the agitation speed 800 rpm. The catalytic reaction was performed at room temperature and lasted for 50 minutes. After the reaction, THF (100 μL) was added as the internal standard for gas chromatographic analysis, followed by high-speed centrifugation to separate the solid catalyst from the liquid phase and the filtrate was determined by GC equipment with a capillary (30 m long $\times$ 0.32 mm i.d., Agilent) and FID detector (Trace 1300, Thermo Scientific, America).

Catalytic Reduction of 4-nitrophenol (4-NP). Typical procedures for the reduction of 4-NP to 4-AP by $NaBH_4$ for testing and comparing the catalytic efficiency with **Pd@NMOF-Ni** and **Pd@MOF-Ni**. Typically, 0.15 mL of 4-NP aqueous solution (0.01 M) and catalysts (2 mg) were added into 11 mL deionized water. The residual air in the reactor was expelled by purging with nitrogen. Subsequently, an aqueous solution of

NaBH$_4$ (1.0 mL, 0.1 M) was introduced to the above system. As can be detected by naked-eyes, initial bright yellow solution gradually faded away as the reaction progressed. The absorbance spectra were used to monitor the reaction progress.
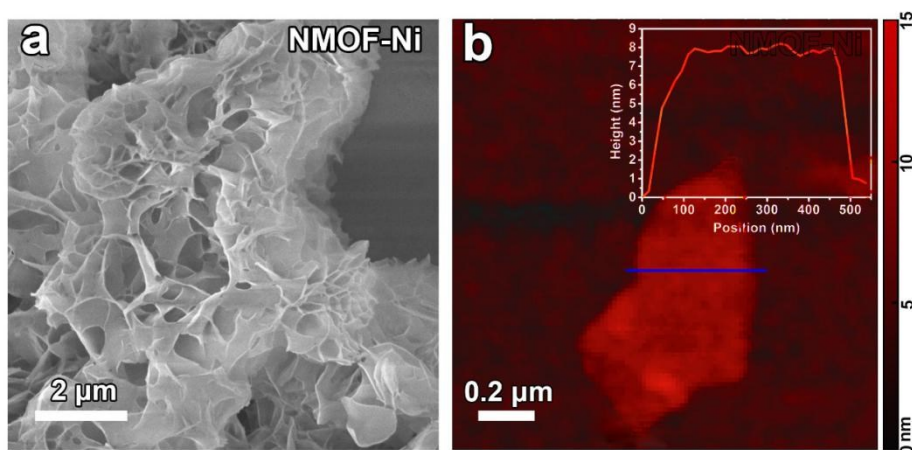
Fig. S1 SEM (a) and AFM (b) image of **NMOF-Ni** nanosheet. (The Inset shows the corresponding height profile of **NMOF-Ni** nanosheets).
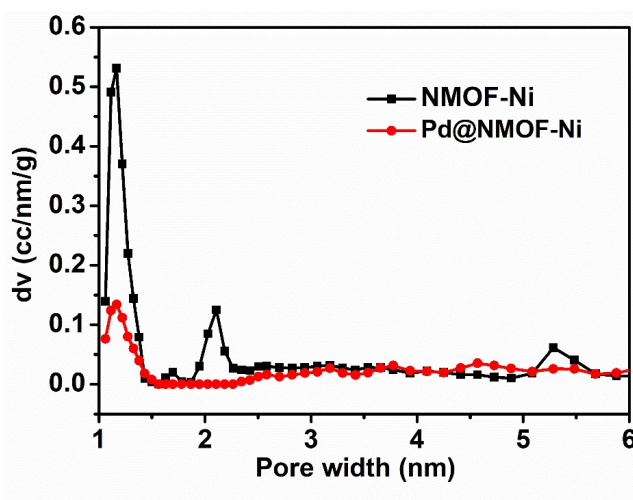
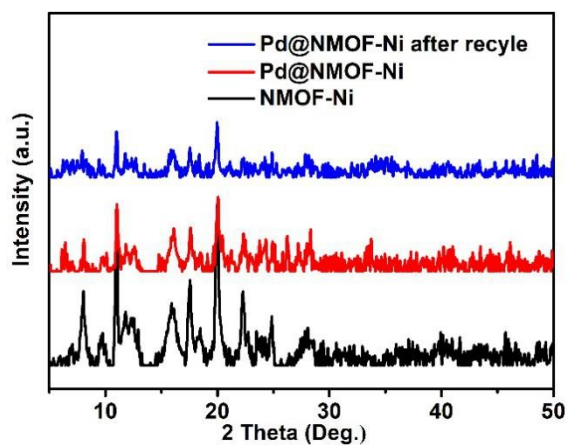**Fig. S2** Pore size distributions of **NMOF-Ni** and **Pd@NMOF-Ni**.
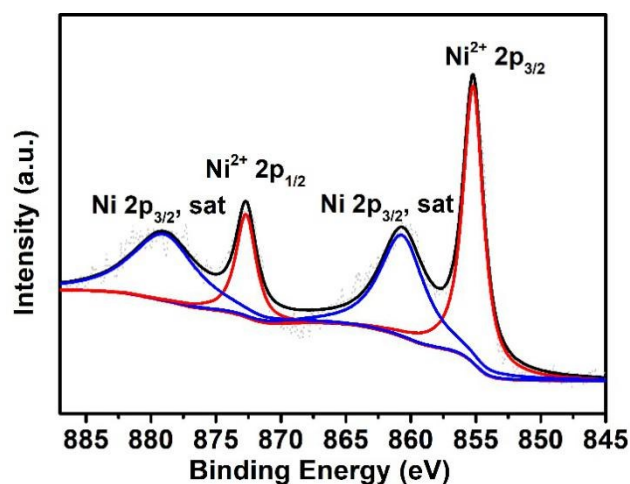
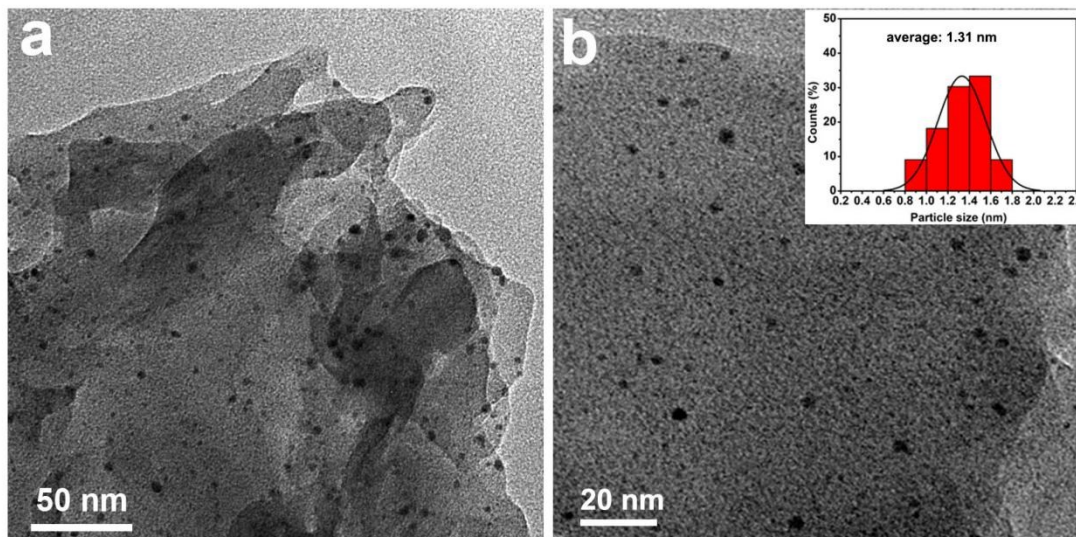**Fig. S3** High-resolution XPS spectrum for Ni^{2+} 2p of **Pd@NMOF-Ni**.

Table S1. Comparison of styrene hydrogenation over different palladium-based catalyst systems.

| Catalyst	Amount	Substrates	T/°C	Time	H$_2$	Yield (%)	TOF/h^{-1}	Reference
Pd@ZIF-8-60	Pd 0.00028 mol%	Pd to substrate molar ratio 1:360	35	240 min	1 atm	89.7	80.81	Chemical Engineering Journal 296 (2016) 146–153
Pd@ZIF-8	Pd 0.127 mol%	alkene 2 mmol	35	720 min	1 atm	100	66.66	J. Mater. Chem. A, 2019, 7, 14504–14509
Void nFe$_3$O$_4$@ZIF-8/Pd@ZIF-8	Pd 0.15 mol%	styrene 0.41 mmol	25	1.5 min	1 atm	100	11600	ACS Appl. Mater. Interfaces 2019, 11, 32251–32260
Void@HKUST-1/Pd@ZIF-8	Pd 0.058 mol%	styrene 0.8mmol	25	5 min	10atm	65	10281	small 2017, 13, 1701395
Pd/Zr-Fc MOF	Pd 0.25 mol%	styrene 0.6 mmol	30	3 min	1atm	99.9	7968	J. Mater. Chem. A, 2019, 7, 15975–15980
Pd@UiO-66-NH$_2$/R	Pd 1 mol%	olefin 0.3 mmol	25	24 h	1 atm	99.5	4.16	Inorg. Chem. Front., 2018,5, 29–38
Pd@MOF-3	Pd 0.6 mol %	alkene 2 mmol	60	300 min	4 atm	99	33.33	Inorg. Chem. 2016, 55, 2345–2354
Pd@ZIF-8 (T)	Pd 0.49 mol%	Olefin 0.4 mmol	35	24 h	1atm	92	8.50	ACS Appl. Mater. Interfaces 2014, 6, 18163–18171
yolk-shell Pd@ZIF-8	Pd 0.08 mol%	alkene 2 mmol	25	24 h	1atm	99	520	CrystEngComm, 2016,18, 1760–1767

|								
Pd-in-UiO-67	Pd 1 mol%	Styrene 0.1 mmol	25	15 min	1atm	100	400	J. Mater. Chem. A, 2015, 3, 15259–15264
Fe$_3$O$_4$@IRMOF-3/Pd	Pd 1 mol%	1. 6 mmol styrene	25	10 min	10atm	>99	594	Chem. Res. Chinese. U. 2016, 37, 573–580.
Pd-NPs@Ln-MOF	Pd 0.059 mol%	styrene 2 mmol	25	420 min	1atm	100	476	J. Mater. Chem. A. 2015, 3, 24525–24531
Pd/MIL-101	Pd 0.43 mol%	styrene 1 mmol	25	60 min	1atm	100	235	J. Nanosci. Nanotechnol. 2014, 14, 2546–2552.
Pd@NMOF-Ni	Pd 0.15 mol%	styrene 0.8 mmol	25	50 min	1atm	100	1230	Our work

**Fig. S4** PXRD patterns of **NMOF-Ni**, **Pd@NMOF-Ni** and **Pd@NMOF-Ni** after recyle.

Fig. S5 TEM images of **Pd@NMOF-Ni** after recycle (The Inset shows the particle size distributions of Pd NPs).
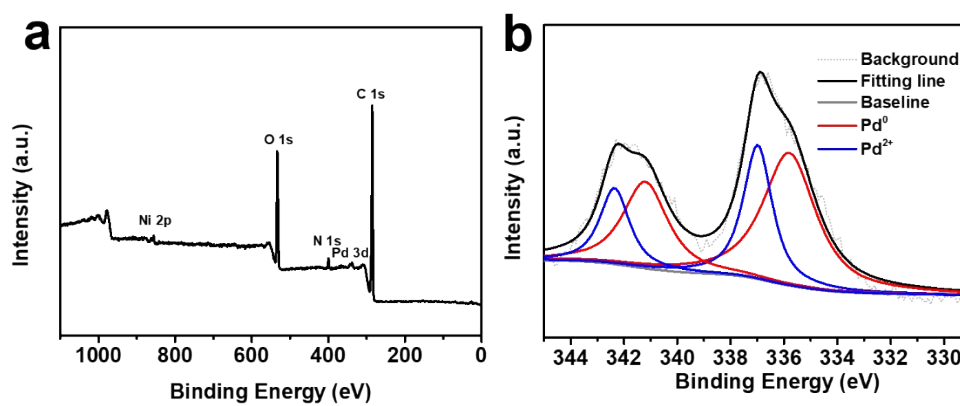
Fig. S6 (a) XPS survey spectra of the used Pd@NMOF-Ni. (b) High-resolution XPS spectrum for Pd 3d of the used Pd@NMOF-Ni.
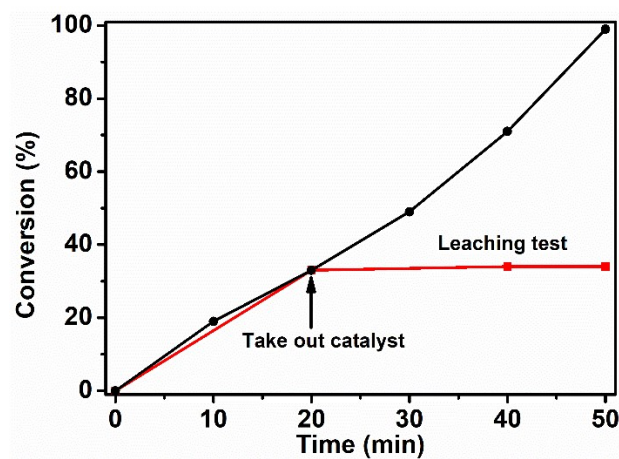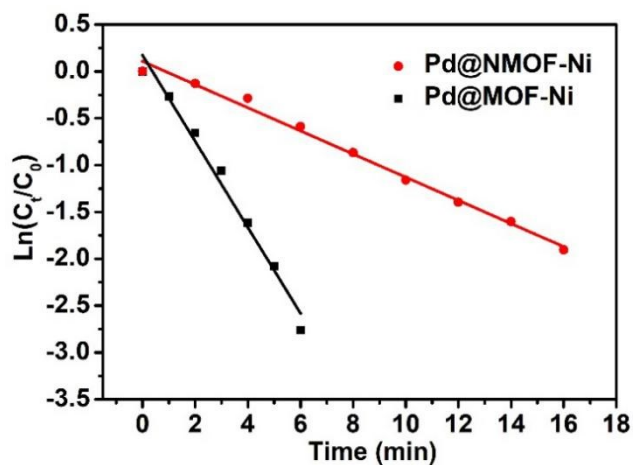
Fig. S7 Leaching tests for the catalytic hydrogenation of styrene over **Pd@NMOF-Ni** under the optimum conditions.
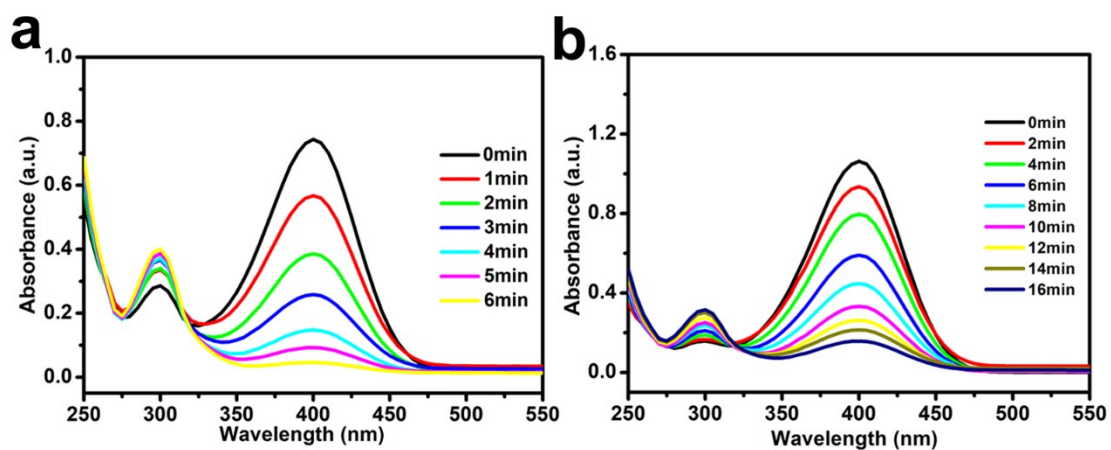
Fig. S8 Representative time-dependent UV–vis adsorption spectra for the catalytic reduction of 4-NP over **Pd@NMOF-Ni** (a), **Pd@MOF-Ni** (b) in aqueous solution at room temperature.

Fig. S9 Relationship of Ln (C_t/C_0) and reaction time for the reduction of 4-NP over **Pd@NMOF-Ni**, and **Pd@MOF-Ni**, where C_0 and C_t are the initial and apparent concentrations of 4-NP, respectively.

Table S2. Estimated kinetic rate constants for the reduction of 4-NP over **Pd@NMOF-Ni**, and **Pd@MOF-Ni** (based on the same Pd content).

	Rate constant (min^{-1})	
Analyte	**Pd@NMOF-Ni**	**Pd@MOF-Ni**
4-NP	4.95×10^{-1}	1.2×10^{-1}

Reference

1 X. B. Shao, X. k. Jiang, X. Z. Wang, Z. T. Li, S. Z. Zhu, *Tetrahedron*, 2003, **59**, 4881−4889.

2 P. Metrangolo, F. Meyer, T. Pilati, D. M. Proserpio, G. Resnati, *Chem. Eur. J.*, 2007, **13**, 5765−5772.

3 R. Yan, Y. Zhao, Hong. Yang, X. J. Kang, C. Wang, L. L. Wen, and Z. D. Lu, *Adv. Funct. Mater.*, 2018, **28**, 1802021.